



Published in final edited form as:

*Nat Chem Biol.* ; 7(9): 624–630. doi:10.1038/nchembio.623.

## CODA-RET reveals functional selectivity as a result of GPCR heteromerization

Eneko Urizar<sup>1,2,5,+</sup>, Hideaki Yano<sup>1,+</sup>, Rachel Kolster<sup>1</sup>, Céline Galés<sup>3</sup>, Nevin Lambert<sup>4</sup>, and Jonathan A. Javitch<sup>1,2,\*</sup>

<sup>1</sup>Center for Molecular Recognition and Departments of Psychiatry and Pharmacology, College of Physicians and Surgeons, Columbia University, 630W. 168th Street, New York, NY 10032

<sup>2</sup>Division of Molecular Therapeutics, New York State Psychiatric Institute, New York, NY 10032, USA

<sup>3</sup>Institut National de la Santé et de la Recherche Médicale, Toulouse, France

<sup>4</sup>Department of Pharmacology and Toxicology, Georgia Health Sciences University, Augusta, 30912-2300

### Abstract

Here we present a novel method that combines protein complementation with resonance energy transfer to study conformational changes in response to activation of a defined G protein-coupled receptor heteromer, and we apply the approach to the putative dopamine D1-D2 receptor heteromer. Remarkably, the potency of the D2 receptor (D2R) agonist R(-)-Propylnorapomorphine (NPA) to change the G $\alpha$ i conformation via the D2R protomer in the D1-D2 heteromer was enhanced 10-fold relative to that observed in the D2R homomer. In contrast, the potencies of the D2R agonists dopamine and quinpirole were the same in the homomer and heteromer. Thus, we have uncovered a molecular mechanism for **functional selectivity**, in which a drug acts differently at a GPCR protomer depending on the identity of the second protomer that participates in forming the signaling unit, opening the door to enhanced pharmacological specificity through targeting differences between homomeric and heteromeric signaling.

### Keywords

GPCR; dopamine; functional selectivity; NPA; dimerization

---

Users may view, print, copy, download and text and data- mine the content in such documents, for the purposes of academic research, subject always to the full Conditions of use: [http://www.nature.com/authors/editorial\\_policies/license.html#terms](http://www.nature.com/authors/editorial_policies/license.html#terms)

\*To whom correspondence should be addressed: J.A.J., jaj2@columbia.edu, Phone: 1-212-305-7308.

<sup>+</sup>These authors contributed equally to the work

<sup>5</sup>Present address: IRIBHM, Brussels, 1170-Belgium.

**Author Contributions:** E.U., H.Y. and R.K. performed experiments; E.U., H.Y. and J.A.J. planned experiments and J.A.J. supervised the project; C.G and N.L provided reagents and discussed the experimental findings and interpretation of results; E.U. and J.A.J. wrote the manuscript.

**Competing Financial Interests:** Authors declare no competing financial interests.

## Introduction

Much evidence suggests that GPCRs are dimeric allosteric machines not only at the level of ligand binding<sup>1</sup> but also of effector activation<sup>2</sup>. Most work to date has been in heterologous systems, and the *in vivo* relevance of dimerization of Class A GPCRs is only beginning to be elucidated<sup>3-7</sup>. Another paradigm shift in the GPCR field relates to the discovery of functional selectivity<sup>8</sup>. The D2 dopamine receptor (D2R) exemplifies a number of aspects of functional selectivity, with substantial differences in potency and efficacy observed for ligands at different signaling readouts<sup>9-11</sup>. Functional selectivity has been proposed to be the basis for the clinical properties of the atypical antipsychotic aripiprazole as well as other drugs<sup>12-14</sup>. Although different receptor conformations must be involved in functional selectivity, there is no clear molecular mechanism that has emerged to date, making it challenging to take advantage of these properties for drug development<sup>8,15</sup>. One possible mechanism for functional selectivity involves heteromerization of receptors with different GPCR partners<sup>8</sup>, and a number of studies have shown that coexpression of two different Class A GPCRs can lead to signaling properties that differ from their properties when expressed alone<sup>16,17</sup>. Importantly, it is not possible from such studies to differentiate downstream integration of signaling from an actual heteromeric signaling unit in which the two protomers interact directly to modulate G protein activation or arrestin recruitment. Indeed, examples of crosstalk by non-interacting GPCRs have been identified<sup>18</sup>, showing the need for caution in interpreting the functional effects of receptor coexpression.

A major obstacle to understanding the functional importance of dimerization between Class A G protein-coupled receptors (GPCRs) has been the methodological limitation in achieving control of the identity of the components comprising the signaling unit. Here, we describe a method we have devised to study heteromeric GPCR signaling without contamination by homomeric species. Based on a technology that combines features of protein complementation<sup>19</sup> and resonance energy transfer<sup>20,21</sup> we are now able to study the function of defined receptor heteromers in living cells in real time. Here we have applied this methodology to the study of the putative dopamine D1R-D2R heteromer<sup>17,22-25</sup>. We demonstrate that norpropylapomorphine (NPA), a high affinity dopamine D2R agonist, binds to D2R and transduces a signal to G $\alpha$ i proteins in a D1R-D2R heteromeric complex with 10-fold higher potency than in the D2R homomer. In contrast, other D2R agonists target the homomer and heteromer with the same potency. Our results indicate that a compound can have distinct effects on signaling as a result of direct receptor-receptor interaction, establishing this as one molecular mechanism for functional selectivity.

## Results

### Measuring receptor activation by receptor-G protein BRET

We first studied dopamine D1 and D2 receptor (D1R and D2R) conformational changes in a BRET-based receptor-G protein assay upon stimulation with the endogenous agonist dopamine (see Supplementary Results section; Supplementary Figure 1, Supplementary Table 1). The BRET<sup>1</sup> assay requires an energy donor, *Renilla Luciferase* 8<sup>26</sup> (RLuc8), fused to the C-terminus of the receptor of interest and an acceptor, mVenus<sup>27</sup>, inserted into the G $\alpha$  subunit at the same position where luciferase was introduced previously<sup>21</sup>. These sensors

have been previously characterized and do not significantly alter the function<sup>19-21</sup> of the wild type (wt) proteins. This technology has been used to monitor conformational changes at the level of the GPCR-G protein interaction for other receptors<sup>20</sup>. Consistent with the known coupling of D1R to G $\alpha$ s, dopamine caused a significant BRET change in cells expressing D1R-RLuc8 with G $\alpha$ s-mVenus but not with G $\alpha$ i-mVenus (Supplementary Figure 1a). This G protein specificity was also observed with another D1R agonist (Supplementary Figure 2a-b, Supplementary Table 1).

Similarly, consistent with the known coupling of D2R to G $\alpha$ i/o, in cells coexpressing D2R-RLuc8 with G $\alpha$ i<sub>1</sub>-mVenus we detected a significant dopamine-induced BRET change, whereas no change in BRET was detected with G $\alpha$ s-mVenus (Supplementary Figure 1b). Other D2R agonists also led to enhancement of the D2R-G protein BRET signal only with G $\alpha$ i-mVenus and not G $\alpha$ s-mVenus (Supplementary Figure 2c-d). We evaluated three different mVenus insertion positions in G $\alpha$ i, and we detected the greatest dynamic range with the insertion at position 91 (Supplementary Figure 2e). Therefore, in all subsequent experiments we used the position 91 G $\alpha$ i-mVenus fusion. Changes in BRET observed with receptor-G protein based biosensors are indicative of conformational change and not necessarily of G protein activation. Importantly, when the sensor is inserted at position 91 of the G $\alpha$ i subunit, the G protein conformational changes have been shown to correlate closely with G protein activation<sup>21</sup>. In order to confirm that the conformational change induced by dopamine also parallels G protein activation, we performed a series of experiments using a G protein biosensor in a configuration that monitors conformational changes at the level of the G protein heterotrimer itself. We expressed a non-tagged receptor (D1R or D2R) together with a G $\alpha$ -RLuc, mVenus-G $\gamma$ <sub>2</sub> and untagged G $\beta$ <sub>1</sub> and we quantified dopamine-induced BRET (Supplementary Figure 1c-d, Supplementary Table 1). As with the receptor-G $\alpha$  based biosensor, we only detected BRET changes when the cognate G $\alpha$  protein was coexpressed along with D1R or D2R (Supplementary Figure 1c-d). Agonist-induced BRET changes were inhibited by specific antagonists (Supplementary Figure 3), consistent with the biosensor reporting on receptor activation.

Thus, as described previously for a BRET<sup>2</sup> assay with adrenergic receptors and related G $\alpha$  biosensors with luciferase or GFP10 inserted at the equivalent of position 91<sup>21</sup>, we were able to use agonist-induced BRET<sup>1</sup> changes to monitor conformational changes that are associated with the activation process. Maximal agonist-induced BRET changes were observed upon coexpression of the G $\alpha$  biosensor together with untagged G $\beta\gamma$  (Supplementary Figure 2f), as previously observed for other receptors<sup>20</sup>.

We obtained similar results with a biosensor that monitored receptor interaction with G $\beta\gamma$ . Here the energy acceptor was a G $\beta\gamma$ -mVenus biosensor, formed by complementation of split mVenus fusion constructs of G $\beta$ <sub>1</sub> and G $\gamma$ <sub>2</sub><sup>28,29</sup> (Supplementary Figure 4), which allows tight control of G $\beta\gamma$  isoforms. Although these biosensors proved robust when coexpressed with receptor fused to RLuc8 and unlabeled G $\alpha$ , a small component of the signal resulted from endogenous G $\alpha$  (Supplementary Figure 4), and therefore this orientation of the assay does not give the same precision when studying conformational changes in a defined G $\alpha$  subunit. Nonetheless, this novel biosensor is of great potential utility as it allows monitoring

conformational changes in defined combinations of G $\beta$  and G $\gamma$  subunits, an aspect of GPCR signaling that is not well understood.

### Expression of D1R alters NPA-induced D2R-G protein BRET

Next we evaluated the impact of receptor coexpression on the agonist induced BRET change. While coexpression of untagged D2R did not alter D1R-dependent G $\alpha_s$  conformational change (Figure 1a), the presence of D1R modified D2R-mediated agonist-induced BRET changes (Figure 1b). Whereas the quinpirole-induced BRET change was not altered in the presence of D1R, we observed a significant gain of potency for R(-)-propylnorapomorphine (NPA) ( $p=0.0001$ , Figure 1b, Table 1), without any change in coupling specificity (Supplementary Figure 2g-h). These data are compatible with the possibility that D1R-D2R heteromerization may be responsible for at least some of the functional selectivity manifested in the ability of different D2R drugs to promote different conformational rearrangements. Although we cannot completely rule out signaling integration resulting from crosstalk of parallel effector pathways, our readout is upstream at the level of the receptor-G protein interaction and not downstream effectors where integration might be more likely.

### Controlling the protomers in a signaling unit

To dissect functional selectivity of D2R drugs at the dimer level, we sought to devise a method that would allow dissection of G protein conformational changes by a defined receptor dimer using receptor sensors recently validated for D2R<sup>19</sup> that exploit complementation of split luciferase as a reporter of molecular proximity<sup>30</sup>. In these constructs the C-terminus of the receptor is fused to an N-terminal fragment (L1) or C-terminal fragment (L2) of RLuc8. We also constructed the equivalent D1R fusion constructs. No differences between D2R-D2R and D2R-D1R were observed when molecular proximity was evaluated by luciferase complementation (Supplementary Figure 5a) or by BRET titration experiments (Supplementary Table 2), suggesting a similar propensity for homo- and heteromerization. Similarly, none of the ligands tested altered the propensity for interaction based on the results of D1R-D2R BRET titration experiments (Supplementary Table 3). Furthermore, none of the drugs targeting one or both receptors altered RLuc8 complementation of the split D2R-D1R or D2R-D2R constructs (Supplementary Figure 5b-c).

Receptor-G protein BRET experiments similar to those described above (Figure 1) were performed in cells that coexpressed D1R-L1 and D1R-L2 or D2R-L1 and D2R-L2 with the G $\alpha_s$  or G $\alpha_i$  mVenus acceptors (Figure 2). Dopamine enhanced the BRET signal in cells that coexpressed D1R-L1, D1R-L2 and G $\alpha_s$ -mVenus (Figure 2a-b, Supplementary Figure 6a-b), but not when the D1R-splits were coexpressed with G $\alpha_i$ -mVenus (Figure 2b), consistent with the expected G protein coupling specificity. G protein specificity also was observed with other D1R agonists (Figure 2c-d). In contrast, G $\alpha_i$  specificity was observed for agonist-induced BRET changes for the complemented D2R-L1 and D2R-L2 splits (Figure 2e-h). Moreover, no significant differences in the potency of dopamine-induced BRET changes were observed between the full length receptor-luciferase fusions and the split luciferase receptor constructs (Table 1, Supplementary Table 1). This indicates not only that the splits

express and function normally, but also that the orientation of the complemented donor is similar and has not introduced an observable alteration of the receptor-G protein interface. As for the full length RLuc8 donor assays, G $\alpha$ i with mVenus inserted at position 91 resulted in the best dynamic range (Supplementary Figure 7a-b) and was used for all subsequent experiments. Importantly, selective drugs did not trigger any BRET change if the target receptor was not expressed (quinpirole in Supplementary Figure 6b). D1R agonists caused concentration-dependent conformational changes in the D1R homomer indicative of G $\alpha$ s activation that are in agreement with the relative potencies and efficacies reported previously using other assays<sup>31</sup> (Figure 2a-d, Supplementary Figure 6b, see Table 1 for quantified potencies). The same was observed for D2R homomer activation of G $\alpha$ i, which identified NPA as the most potent agonist studied (Figure 2e-h, Table 1). Comparable results were observed when we used the G $\beta\gamma$ -mVenus or G $\gamma$ -mVenus biosensors for D2R homomers (Supplementary Figure 8, Supplementary Table 1).

As expected, selective antagonists dramatically decreased agonist potency at the cognate receptor. In cells coexpressing the D1R splits and G $\alpha$ s-mVenus, the D1R antagonist SCH23390 decreased the potency of dopamine, DAR100 and SKF83822 for activating G $\alpha$ s (Figure 2b, Supplementary Figure 6c-d); and the D2R antagonist sulpiride decreased the potency of dopamine, NPA and quinpirole for activating G $\alpha$ i (Figure 2f, Supplementary Figure 7c-d). In contrast, SCH23390 did not inhibit NPA- or quinpirole-induced BRET increase in D2R G $\alpha$ i-mVenus expressing cells (Supplementary Figure 7c-f). Notably the D2R-selective antagonist sulpiride has a fixed negative charge and at 1  $\mu$ M is essentially membrane impermeant<sup>32</sup>. Therefore, the dramatic inhibition of the agonist-induced BRET change by this concentration of sulpiride in cells coexpressing the D2R splits and G $\alpha$ i-mVenus, (Figure 2f, Supplementary Figure 7c-f), indicates that essentially all of the agonist-induced BRET changes take place at the plasma membrane.

### Targeting the D1R-D2R heteromeric signaling unit

This approach allows targeting of specific protomers through luciferase complementation and thus analysis of signaling of defined heteromers without a contribution from homomeric complexes. Thus, by coexpressing D1R-L1 and D2R-L2 (or D2R-L1 and D1R-L2), the only luminescence signal will result from complementation of D1R and D2R and any homomeric species will be silent at the level of the BRET readout. We first studied the G $\alpha$ s pathway by coexpressing both D2R-L1 and D1R-L2 with G $\alpha$ s-mVenus. Selective D1R stimulation resulted in a concentration-dependent BRET increase with agonist potencies similar to those observed in the D1R homomers (Figure 3a-d, Supplementary Figure 6e-f, Table 1, Supplementary Table 1). The D2R-specific agonist quinpirole did not alter the G $\alpha$ s-mVenus BRET signal (Supplementary Figure 6f). Furthermore, as expected, the selective D1R inhibitor SCH23390 competed with the D1R-selective compounds, whereas the D2R-selective antagonist sulpiride did not inhibit the D1R-mediated G $\alpha$ s response (Figure 3a-d). Selective antagonism by SCH23390 was also seen for DAR100 (Supplementary Figure 6g-h). Swapping the orientation of the splits led to the same results (Supplementary Figure 9a). This set of experiments demonstrates that, agonist binding to the D1R protomer in a D1R-D2R complex is sufficient to trigger a conformational change between the heteromer and G $\alpha$ s consistent with activation. This establishes that one agonist is sufficient to activate a

receptor heteromer. Moreover, since our approach monitors the direct physical interaction between the receptor heteromer and G $\alpha$  protein, downstream signaling crosstalk is very unlikely to contribute to the observed BRET changes.

### Functional selectivity of NPA at the D2R-D1R heteromer

Next, we studied the G $\alpha_i$  pathway by coexpressing D2R-L1 and D1R-L2 with G $\alpha_i$ -mVenus. Again D2R agonists led to BRET increases similar to those observed in the D2R homomers (Figure 3e-h, Table 1). Swapping the splits led to comparable results with the same potency for quinpirole (Supplementary Figure 8b, Supplementary Table 1). As expected, agonist-induced BRET was inhibited by the D2R antagonist sulpiride (Figure 3e-h), but not by the D1R antagonist SCH23390 (Figure 3e-h). Thus, agonist binding to the D2R in the heteromer triggers a conformational change in the D2R-D1R-G $\alpha_i$  signaling complex.

With G $\alpha_s$  and the complemented donors, we detected no difference in potency between the D1R homomer and D1R-D2R heteromer for any of the D1R agonists tested (Figure 4a, Supplementary Figure 9a, Table 1 and Supplementary Table 1). Likewise, with G $\alpha_i$  the potencies of quinpirole and dopamine to enhance BRET were the same in the complemented D2R homomer and the D1R-D2R heteromer (Figure 4b). In contrast, in agreement with the increased potency for the NPA induced BRET change in D2R-RLuc8 G $\alpha_i$ -mVenus in the presence of untagged D1R (Figure 1b, Table 1), NPA was approximately 10-fold more potent at the heteromer than at the D2R homomer ( $p < 0.005$ , Figure 4b, Table 1). These results provide evidence for a novel molecular mechanism for functional selectivity, by which a drug has different potencies when targeting homo- or heteromeric complexes.

Since NPA also binds and activates D1R, it is conceivable that NPA binding to the D1R protomer in the heteromer might help to *trans*-activate G $\alpha_i$  and thereby enhance NPA's potency, but our results suggest otherwise. The NPA-induced BRET change with the D2R-D1R-G $\alpha_i$  sensor was competed by the D2R-inhibitor sulpiride but not by the D1R-inhibitor SCH23390 (Figure 3h), suggesting that NPA activates G $\alpha_i$  only by binding to the D2R and not to the D1R. In addition, whereas complementation of a mutant D2R that does not bind agonist<sup>33</sup> (D2R-D114A-L1) with D1R produced a heteromer that signaled normally to G $\alpha_s$ , neither NPA, quinpirole, nor dopamine signaled to G $\alpha_i$  (Supplementary Figure 10), indicating the binding to the D2R protomer is essential for G $\alpha_i$  activation.

Importantly, expression of excess unlabelled D1R did not alter the ability of the D2R-D2R splits to activate G $\alpha_i$  (Supplementary Figure 11a-b) and failed to allow the D2R-D2R splits to activate G $\alpha_s$  (Supplementary Figure 11e-g). Similarly, expression of unlabeled D2R did not impact the ability of the D1R-D1R splits to activate G $\alpha_s$  (Supplementary Figure 11c-d) and failed to produce activation of G $\alpha_i$  (Supplementary Figure 11h-j). These critical controls establish that the biosensors only read out on the activity of the receptor protomers to which they are directly fused.

## Discussion

We have developed a new methodology that allows the study of a signaling complex comprised of two defined GPCRs. This technology is based on quantifying the BRET



between a receptor heteromer and a subunit of the heterotrimeric G protein. Receptor-receptor interaction generates a complemented luminescence signal<sup>34</sup> that serves as the energy donor of the assay. This creates tight control of the receptor species that participate in the energy transfer, allowing us to measure communication between a defined pair of receptor protomers and the G protein of choice, without contamination by homomeric signaling complexes or downstream crosstalk. Indeed, when studying heteromers with this methodology, homomers are “left in the dark,” since the formation of homomeric receptor complexes do not result in luminescence and therefore cannot contribute a signal in the BRET assay. We term this approach **Complemented Donor Acceptor resonance energy transfer (CODA-RET)** to emphasize that it reports on interactions involving three or four entities. Importantly, this approach can also be used to explore the ability of defined receptor heteromers to recruit arrestin and can be extended to different interacting partners, as well as to FRET-based assays, by substituting split green fluorescent protein variants for the split luciferase constructs used here.

In heterologous cells and in *ex vivo* systems, coexpression of two receptors has often been shown to lead to an alteration in pharmacology, trafficking, or generation of distinct downstream signals that differ from the properties of the individual receptors<sup>7,35,36</sup>. Although this is often taken as evidence of altered signaling by heteromers composed of the two different receptors, downstream crosstalk could also account for these findings. Even in cases where physical proximity is demonstrated between receptors with energy transfer assays, it is still not justified to conclude that signaling comes from the heteromer, as a fraction of the receptors may indeed interact, particularly in heterologous systems, but the functional entities may be the individual receptors or homomers interacting through downstream crosstalk. When two Class A receptors are coexpressed, homomeric and heteromeric species are likely to exist, and signaling could result from any combination of these receptor complexes<sup>37,38</sup>. Distinguishing between direct signaling from heteromers and indirect crosstalk downstream of homomers is of more than semantic importance. Given the opportunity for allosteric modulation between protomers in a heteromeric signaling unit<sup>1,2,7</sup>, novel drugs might be developed that would act differently at a heteromer than at a homomer, whereas with downstream crosstalk one would pursue a different pharmacological strategy to regulate signaling crosstalk.

Certain compounds can differentially modulate various downstream signaling pathways upon binding to the same receptor<sup>15</sup>. This functional selectivity<sup>39</sup> can manifest in different relative potencies of a drug at different downstream signaling<sup>40,41</sup> or in the same molecule regulating different pathways in an opposite direction<sup>42</sup>. Although this phenomenon is generally believed to result from different distributions of receptor conformations resulting from binding different ligands, our understanding of the underlying molecular mechanisms are quite limited. We have demonstrated here using CODA-RET that receptor heteromerization can result in functional selectivity, and we are able to establish for the first time that this functional selectivity results at the level of direct interaction of the heteromer with G protein and not as a result of downstream crosstalk.

NPA, a high affinity D2R agonist caused an unexpected and previously undocumented higher potency conformational rearrangement of the G $\alpha$ i protein in the D2R-D1R heteromer

when compared to the D2R-D2R homomer. This is a clear example of functional selectivity because dopamine and quipirole showed no significant shift in potency at the two complexes. The inability of the D1R antagonist SCH23390 to block NPA-induced G $\alpha$ i BRET changes, and the loss of NPA-induced conformational changes upon mutation of the D2R binding site or in the presence of the specific D2R inverse agonist sulpiride, indicated that in the D1R-D2R heteromer the higher potency of NPA for G $\alpha$ i *only* required its binding to the D2R and not to D1R.

We have previously shown that complementation of receptor RLuc split constructs does not increase the interaction of the complemented receptors in the plasma membrane based on independent measurement of energy transfer between extracellular epitopes<sup>19</sup>. Furthermore, because the potency of NPA was enhanced similarly for the D1R-L1-D2R-L2 complemented complex and the D2R full-length RLuc8 fusion coexpressed with D1R, we conclude that the alteration in potency results not from the impact of complementation but rather from receptor-receptor interaction. Thus, the ability to monitor G protein conformational changes selectively in a defined heteromer using CODA-RET should allow for more precise dissection of heteromeric signaling. A number of findings suggest that GPCR dimerization in the plasma membrane may be transient<sup>43-45</sup>. Even if GPCR interactions are transient, the substantial time the receptors spend together<sup>43</sup> is likely sufficient for the types of allosteric modulation between receptors that have been described<sup>1,2,7</sup> and that can be revealed by CODA-RET.

The molecular mechanism of the enhanced potency of NPA remains to be determined. The presence of the D1R in the heteromer somehow may exert an allosteric effect that modifies the binding site of the D2R and/or the mechanism by which agonist binding is propagated to G protein conformational rearrangement. A second nonexclusive possibility is that the cytoplasmic face of the D1R somehow contributes directly to the activation of G $\alpha$ i mediated by the agonist-bound D2R protomer in the heteromer, as has been inferred for the D2R homomer<sup>2</sup>. It is not yet clear that this specific example of functional selectivity is manifested downstream of the change in G $\alpha$ i conformation. Our efforts to investigate downstream signaling of this particular heteromer have been complicated by the competing effects on downstream signaling of G $\alpha$ i and G $\alpha$ s activation by D2R and D1R and by our inability to assay selectively the effectors activated by the heteromeric and not homomeric complexes, which could mask the signal from a subset of heteromeric complexes.

In summary, our finding that the identity of the receptor partner in a GPCR heteromer can selectively alter the potency of agonist-induced signaling to G proteins indicates that receptor heteromerization is an important factor that must be considered in drug design and pharmacological analysis. Whether this is a general mechanism that can be exploited to develop new compounds selectively targeting D1R-D2R or other GPCR heteromers remains to be tested, but CODA-RET allows an approach to eliminating a contribution from homomeric signaling and analyzing the effect of drugs on defined GPCR heteromers.



## Material and Methods

### Constructs for expression vectors and transfection

The cDNA for human D1R was obtained from [www.cdna.org](http://www.cdna.org). D1R was tagged with signal peptide (SP) followed<sup>46</sup> by a Myc epitope tag using standard molecular biology procedures. The cDNAs encoding full length *Renilla Luciferase* 8 (RLuc8) or fragments for the L1 (residues 1-229) or L2 (residues 230-311) were fused in frame to the C terminus of D1R in the pcDNA3.1 vector. The human D2<sub>short</sub>R sensors were already reported<sup>19</sup>. The following human G protein constructs were used: untagged G $\alpha_{i1}$  and long Gas, G $\alpha_{i1}$ -mVenus with mVenus inserted at position 60, 91, or 122, long Gas-mVenus with mVenus inserted at position 71 (aligned with position 60 in G $\alpha_{i1}$ ), G $\alpha_{i1}$ -RLuc (humanized regular *Renilla Luciferase*) inserted at position 91, Gas-RLuc with RLuc inserted at position 113, untagged G $\beta_1$ , G $\beta_1$  fused with V2 (C terminal split of mVenus, aa 156-240) at its N-terminus, untagged G $\gamma_2$ , G $\gamma_2$  fused with V1 (N terminal split of mVenus, aa 1-155) at its N-terminus, G $\gamma_2$  fused to full-length mVenus at its N-terminus. All the constructs were confirmed by sequencing analysis.

A constant amount of plasmid cDNA was transfected into HEK-293T cells using polyethylenimine (PEI) (Polysciences Inc) in a 1 to 3 ratio in 10 cm dishes. Cells were maintained in culture with DMEM supplemented with 10% FBS. The transfected amount and ratio among the receptor-L1, receptor-L2, G $\alpha$ , G $\beta_1$ , G $\gamma_2$  was optimized by testing various ratios of plasmids encoding the different sensors. Experiments were performed ~48 hours post-transfection.

### BRET

BRET<sup>1</sup>, which differs from other forms of BRET (BRET<sup>2</sup> and BRET<sup>3</sup>) in that it uses a yellow fluorescent protein as an acceptor for energy transfer from luciferase, were performed as described<sup>19,47</sup>. Briefly, cells were harvested, washed and resuspended in PBS. Approximately 200,000 cells/well were distributed in 96-well plates and 5  $\mu$ M coelenterazine H (substrate for luciferase) was added to each well. One min after addition of coelenterazine H ligands were added to each well and immediately after the addition, the fluorescence (excitation at 500 nm and emission at 540 nm, 1s recording) and luminescence after substrate addition (no filters, 1s recording) were quantified (Polarstar and Pherastar, respectively, BMG). In parallel cells the BRET signal was determined by quantifying and calculating the ratio of the light emitted by mVenus (510–540 nm) over that emitted by RLuc8 or RLuc (485 nm) for BRET<sup>1</sup>. The net BRET values were obtained by subtracting the background determined in cells expressing RLuc8 or RLuc alone. Results are expressed as the BRET change produced by the corresponding drug. As shown in the cartoons, bimolecular complementation of donor was incorporated into the BRET assay. In a majority of the combinations tested, luminescence resulted from bimolecular luminescence complementation between D2R-L1 and D1R-L2 and RET took place between that complex and G $\alpha$ -mVenus. Data and statistical analysis were performed with Prism 5.01 (GraphPad Software).

## FACS Analysis

FACS was performed to determine surface expression of each receptor construct, as described<sup>48</sup> with the Guava Easy Cite cytometer (Guava Technologies) or C6 Flow Cytometer (Accuri). Briefly, a fraction of the same cells used for luminescence complementation was harvested and incubated with anti-Flag (Sigma) or anti-Myc (Hybridoma Facility, Mount Sinai, New York), washed and incubated with secondary antimouse antibody labelled with Alexa Fluor 647 (Invitrogen).

## Drugs

Pharmacological reagents were purchased from following vendors: dopamine (Sigma), quinpirole (Sigma), R(-)-Propylnorapomorphine (NPA) (Sigma), dihydrexidine (DAR-100) (Tocris), SKF38393 (Sigma), SKF81297 (Tocris), SKF83822 (Tocris), sulpiride (Sigma), SCH23390 (Sigma). Each ligand was solubilized in a corresponding solvent (e.g. methanol, ethanol, and DMSO) and non-ligand control contained the same amount of solvent to address potential solvent effects on the BRET assay.

## Supplementary Material

Refer to Web version on PubMed Central for supplementary material.

## Acknowledgments

This work was supported in part by NIH grants DA022413 and MH054137 (J.A.J.), GM078319 (N.L.), NIH TL1 RR024158-04 (H.Y.), the Lieber Center for Schizophrenia Research and Treatment, and an EMBO Long term and Basque Country fellowships (E.U.).

## Reference List

1. Springael JY, Urizar E, Costagliola S, Vassart G, Parmentier M. Allosteric properties of G protein-coupled receptor oligomers. *Pharmacology & Therapeutics*. 2007; 115:410–418. [PubMed: 17655934]
2. Han Y, Moreira IS, Urizar E, Weinstein H, Javitch JA. Allosteric communication between protomers of dopamine class A GPCR dimers modulates activation. *Nat Chem Biol*. 2009; 5:688–695. [PubMed: 19648932]
3. Ferre S, et al. Building a new conceptual framework for receptor heteromers. *Nat Chem Biol*. 2009; 5:131–134. [PubMed: 19219011]
4. Albizu L, et al. Time-resolved FRET between GPCR ligands reveals oligomers in native tissues. *Nat Chem Biol*. 2010; 6:587–594. [PubMed: 20622858]
5. Rivero-Muller A, et al. Rescue of defective G protein-coupled receptor function in vivo by intermolecular cooperation. *Proc Natl Acad Sci U S A*. 2010; 107:2319–2324. [PubMed: 20080658]
6. Milligan G. G protein-coupled receptor hetero-dimerization: contribution to pharmacology and function. *Br J Pharmacol*. 2009; 158:5–14. [PubMed: 19309353]
7. Smith NJ, Milligan G. Allostery at G Protein-Coupled Receptor Homo- and Heteromers: Uncharted Pharmacological Landscapes. *Pharmacol Rev*. 2010; 62:701–725. [PubMed: 21079041]
8. Urban JD, et al. Functional Selectivity and Classical Concepts of Quantitative Pharmacology. *J Pharmacol Exp Ther*. 2007; 320:1–13. [PubMed: 16803859]
9. Kilts JD, et al. Functional Selectivity of Dopamine Receptor Agonists. II. Actions of Dihydrexidine in D2L Receptor-Transfected MN9D Cells and Pituitary Lactotrophs. *J Pharmacol Exp Ther*. 2002; 301:1179–1189. [PubMed: 12023553]

10. Masri B, et al. Antagonism of dopamine D2 receptor/beta-arrestin 2 interaction is a common property of clinically effective antipsychotics. *PNAS*. 2008; 105:13656–13661. [PubMed: 18768802]
11. Mottola DM, et al. Functional Selectivity of Dopamine Receptor Agonists. I. Selective Activation of Postsynaptic Dopamine D2 Receptors Linked to Adenylate Cyclase. *J Pharmacol Exp Ther*. 2002; 301:1166–1178. [PubMed: 12023552]
12. Mailman RB. GPCR functional selectivity has therapeutic impact. *Trends in Pharmacological Sciences*. 2007; 28:390–396. [PubMed: 17629962]
13. Urban JD, Vargas GA, von Zastrow M, Mailman RB. Aripiprazole has Functionally Selective Actions at Dopamine D2 Receptor-Mediated Signaling Pathways. *Neuropsychopharmacology*. 2006; 32:67–77. [PubMed: 16554739]
14. Bosier B, Hermans E. Versatility of GPCR recognition by drugs: from biological implications to therapeutic relevance. *Trends in Pharmacological Sciences*. 2007; 28:438–446. [PubMed: 17629964]
15. Kenakin T. Collateral efficacy in drug discovery: taking advantage of the good (allosteric) nature of 7TM receptors. *Trends in Pharmacological Sciences*. 2007; 28:407–415. [PubMed: 17629960]
16. George SR, et al. Oligomerization of mu- and delta-opioid receptors - Generation of novel functional properties. *J Biol Chem*. 2000; 275:26128–26135. [PubMed: 10842167]
17. Lee SP, et al. Dopamine D1 and D2 Receptor Co-activation Generates a Novel Phospholipase C-mediated Calcium Signal. *J Biol Chem*. 2004; 279:35671–35678. [PubMed: 15159403]
18. Rives ML, et al. Crosstalk between GABA(B) and mGlu1a receptors reveals new insight into GPCR signal integration. *EMBO J*. 2009; 28:2195–2208. [PubMed: 19590495]
19. Guo W, et al. Dopamine D2 receptors form higher order oligomers at physiological expression levels. *EMBO J*. 2008; 27:2293–2304. [PubMed: 18668123]
20. Gales C, et al. Real time monitoring of receptor and G-protein interactions in living cells. *Nature Methods*. 2005; 2:177–184. [PubMed: 15782186]
21. Gales C, et al. Probing the activation-promoted structural rearrangements in preassembled receptor-G protein complexes. *Nature Structural & Molecular Biology*. 2006; 13:778–786.
22. O'Dowd BF, et al. Dopamine Receptor Oligomerization Visualized in Living Cells. *J Biol Chem*. 2005; 280:37225–37235. [PubMed: 16115864]
23. Rashid AJ, et al. D1-D2 dopamine receptor heterooligomers with unique pharmacology are coupled to rapid activation of Gq/11 in the striatum. *PNAS*. 2007; 104:654–659. [PubMed: 17194762]
24. So CH, et al. D1 and D2 Dopamine Receptors Form Heterooligomers and Cointernalize after Selective Activation of Either Receptor. *Mol Pharmacol*. 2005; 68:568–578. [PubMed: 15923381]
25. So CH, Verma V, O'Dowd BF, George SR. Desensitization of the Dopamine D1 and D2 Receptor Hetero-Oligomer Mediated Calcium Signal by Agonist Occupancy of Either Receptor. *Mol Pharmacol*. 2007; 72:450–462. [PubMed: 17519357]
26. Loening AM, Fenn TD, Wu AM, Gambhir SS. Consensus guided mutagenesis of Renilla luciferase yields enhanced stability and light output. *Protein Eng*. 2006; 19:391–400.
27. Nagai T, et al. A variant of yellow fluorescent protein with fast and efficient maturation for cell-biological applications. *Nat Biotech*. 2002; 20:87–90.
28. Hynes TR, et al. Visualization of G Protein betagamma Dimers Using Bimolecular Fluorescence Complementation Demonstrates Roles for Both beta and gamma in Subcellular Targeting. *J Biol Chem*. 2004; 279:30279–30286. [PubMed: 15136579]
29. Mervine SM, Yost EA, Sabo JL, Hynes TR, Berlot CH. Analysis of G Protein beta{gamma} Dimer Formation in Live Cells Using Multicolor Bimolecular Fluorescence Complementation Demonstrates Preferences of beta1 for Particular {gamma} Subunits. *Mol Pharmacol*. 2006; 70:194–205. [PubMed: 16641313]
30. Paulmurugan R, Umezawa Y, Gambhir SS. Noninvasive imaging of protein-protein interactions in living subjects by using reporter protein complementation and reconstitution strategies. *PNAS*. 2002; 99:15608–15613. [PubMed: 12438689]
31. Zhang J, Xiong B, Zhen X, Zhang A. Dopamine D1 receptor ligands: where are we now and where are we going. *Med Res Rev*. 2009; 29:272–294. [PubMed: 18642350]

32. Guo N, et al. Impact of D2 Receptor Internalization on Binding Affinity of Neuroimaging Radiotracers. *Neuropsychopharmacology*. 2009; 35:806–817. [PubMed: 19956086]
33. Mansour A, et al. Site-directed mutagenesis of the human dopamine D2 receptor. *Eur J Pharmacol*. 1992; 227:205–214. [PubMed: 1358663]
34. Paulmurugan R, Gambhir SS. Monitoring protein-protein interactions using split synthetic renilla luciferase protein-fragment-assisted complementation. *Analytical Chemistry*. 2003; 75:1584–1589. [PubMed: 12705589]
35. Terrillon S, Bouvier M. Roles of G-protein-coupled receptor dimerization - From ontogeny to signalling regulation. *Embo Reports*. 2004; 5:30–34. [PubMed: 14710183]
36. Dalrymple MB, Pflieger KDG, Eidne KA. G protein-coupled receptor dimers: Functional consequences, disease states and drug targets. *Pharmacology & Therapeutics*. 2008; 118:359–371. [PubMed: 18486226]
37. Selbie LA, Hill SJ. G protein-coupled-receptor cross-talk: the fine-tuning of multiple receptor-signalling pathways. *Trends in Pharmacological Sciences*. 1998; 19:87–93. [PubMed: 9584624]
38. Bygrave FL, Roberts HR. Regulation of cellular calcium through signaling cross-talk involves an intricate interplay between the actions of receptors, G-proteins, and second messengers. *FASEB J*. 1995; 9:1297–1303. [PubMed: 7557019]
39. Kenakin T. Agonist-Receptor Efficacy. 2. Agonist Trafficking of Receptor Signals. *Trends in Pharmacological Sciences*. 1995; 16:232–238. [PubMed: 7667897]
40. Meller E, Puza T, Diamond J, Lieu HD, Bohmaker K. Comparative effects of receptor inactivation, 17 beta-estradiol and pertussis toxin on dopaminergic inhibition of prolactin secretion in vitro. *J Pharmacol Exp Ther*. 1992; 263:462–469. [PubMed: 1359107]
41. Spengler D, et al. Differential signal transduction by five splice variants of the PACAP receptor. *Nature*. 1993; 365:170–175. [PubMed: 8396727]
42. Wisler JW, et al. A unique mechanism of beta-blocker action: Carvedilol stimulates beta-arrestin signaling. *PNAS*. 2007; 104:16657–16662. [PubMed: 17925438]
43. Hern JA, et al. Formation and dissociation of M1 muscarinic receptor dimers seen by total internal reflection fluorescence imaging of single molecules. *PNAS*. 2010; 107:2693–2698. [PubMed: 20133736]
44. Fonseca JM, Lambert NA. Instability of a Class A G Protein-Coupled Receptor Oligomer Interface. *Mol Pharmacol*. 2009; 75:1296–1299. [PubMed: 19273553]
45. Dorsch S, Klotz KN, Engelhardt S, Lohse MJ, Bunemann M. Analysis of receptor oligomerization by FRAP microscopy. *Nat Meth*. 2009; 6:225–230.
46. Guo W, Shi L, Javitch JA. The Fourth Transmembrane Segment Forms the Interface of the Dopamine D2 Receptor Homodimer. *J Biol Chem*. 2003; 278:4385–4388. [PubMed: 12496294]
47. Urizar E, et al. Glycoprotein hormone receptors: link between receptor homodimerization and negative cooperativity. *Embo Journal*. 2005; 24:1954–1964. [PubMed: 15889138]
48. Costagliola S, Khoo D, Vassart G. Production of bioactive amino-terminal domain of the thyrotropin receptor via insertion in the plasma membrane by a glycosylphosphatidylinositol anchor. *Febs Letters*. 1998; 436:427–433. [PubMed: 9801163]

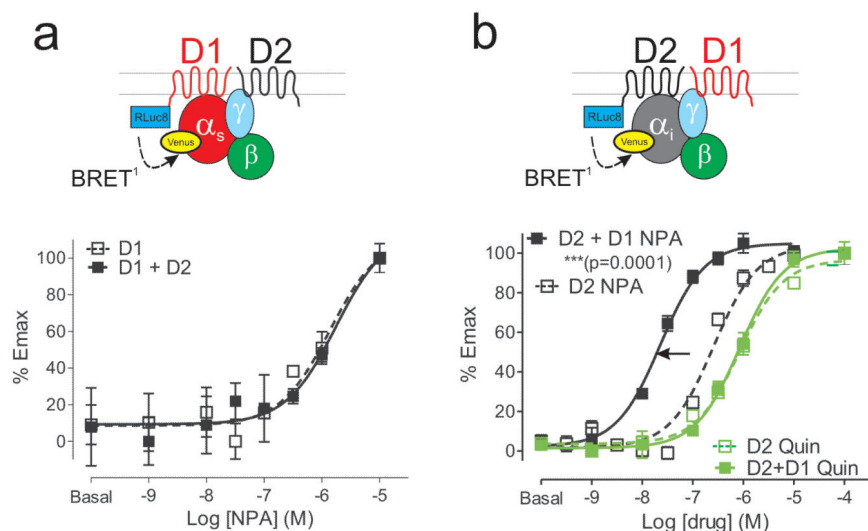


**Figure 1. D1R coexpression enhances NPA potency at D2R**

HEK 293T cells transiently expressing wild type human D1R (a) or D2R (b) full length RLuc8 C-terminal fusions alone or in combination with unfused D2R (a) or D1R (b) respectively; together with  $G_{\alpha s}$ -mVenus (a) or  $G_{\alpha i}$ -mVenus (b) and unfused  $\beta_1$  and  $\gamma_2$  G protein subunits were harvested 48 h post-transfection, washed with PBS, centrifuged and resuspended in PBS. Cells were distributed in 96-well plates and preincubated with coelenterazine H for 1 min and then with increasing concentrations of dopamine for 1 min. BRET<sup>1</sup> was performed as described in Materials and Methods and results were fit by non-linear regression to a sigmoidal dose-response relationship against the agonist concentration. The graphs are representative of 2-12 independent experiments performed with triplicate samples (error bars represent S.E.M), and summary data are presented in Table 1. The cartoons indicate the constructs expressed: D1R in red and D2R in black with the full length RLuc8 (blue) at the C terminus and the indicated  $G_{\alpha}$  sensor (red for  $G_{\alpha s}$  or black for  $G_{\alpha i}$ ) with the  $\beta_1$  (in green) and  $\gamma_2$  (in light blue) subunits; the dotted arrow represents the energy transfer.

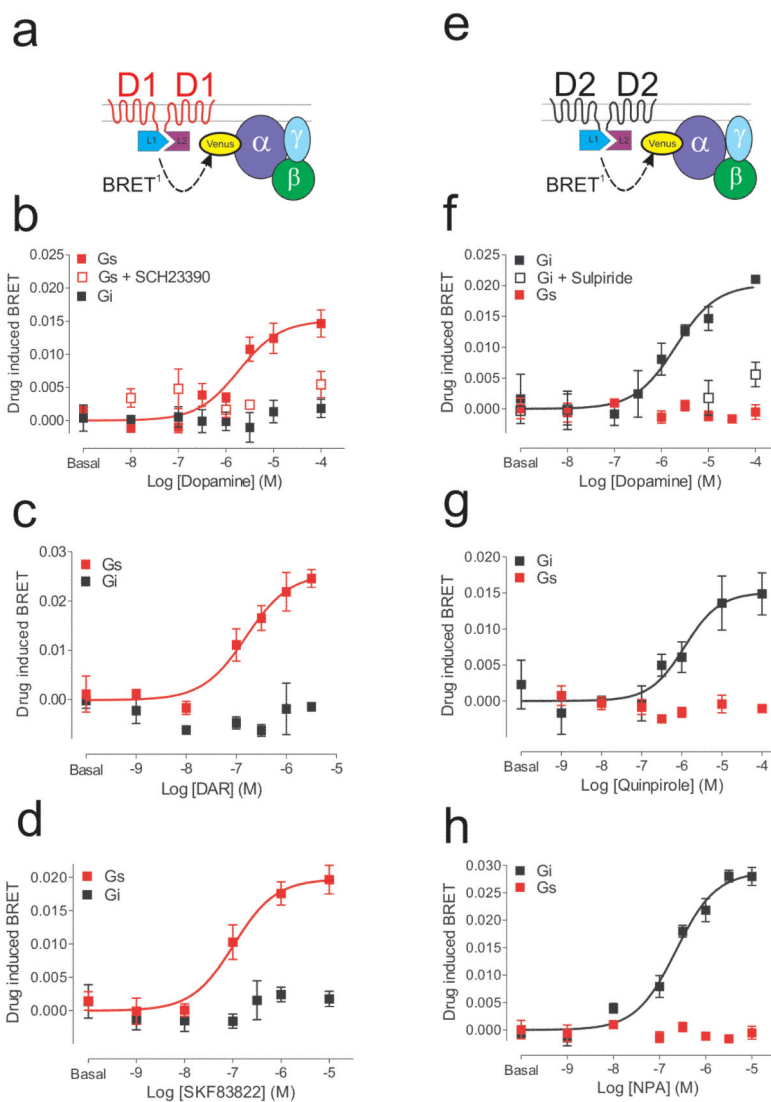


**Figure 2. Characterization of homomeric receptors in G protein signaling complexes** HEK 293T cells coexpressing D1R-L1, D1R-L2 and G $\alpha$ s-mVenus (red symbols and curves) or G $\alpha$ i-mVenus (black symbols and curves) (a-d) or D2R-L1, D2R-L2 and G $\alpha$ i-mVenus (black symbols and curves) or G $\alpha$ s-mVenus (red symbols) (e-h) were prepared as in Figure 1. In experiments in which antagonists (SCH23390, sulpiride) were used (b, f open symbols), the antagonists (1  $\mu$ M) were preincubated for 15 mins at RT before the addition of the substrate and the tested agonist. BRET<sup>1</sup> was measured as explained in Material and Methods and analyzed as for Figure 1. The graphs are representative of 2-12 independent experiments performed with triplicate samples (error bars represent S.E.M), and summary data are presented in Table 1.



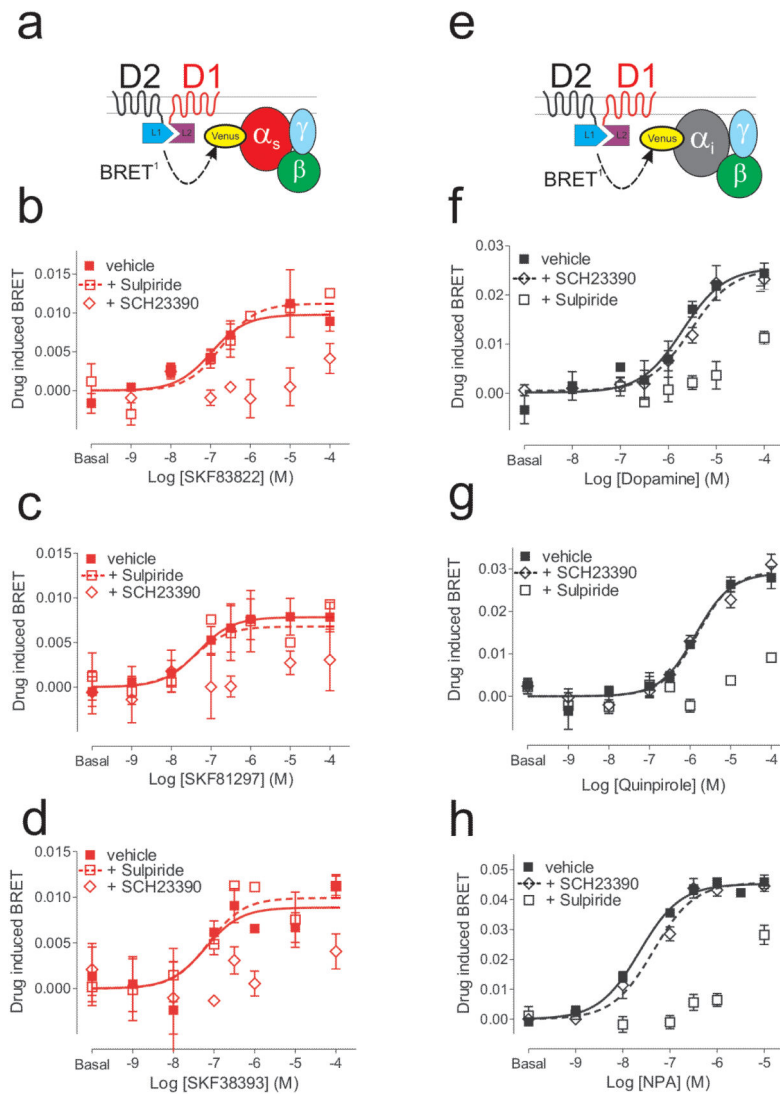


**Figure 3. Characterization of the heteromeric receptors in G protein signaling complexes** HEK 293T cells coexpressing D2R-L1, D1R-L2 and G $\alpha_s$ -mVenus (**a-d**) or G $\alpha_i$ -mVenus (**e-h**) were prepared as described in Figure 1. In experiments in which antagonists were used (open symbols), the antagonists (1  $\mu$ M) were preincubated for 15 mins at RT before the addition of the substrate and the tested agonist. BRET<sup>1</sup> was measured as explained in Material and Methods and analyzed as for Figure 1. The graphs are representative of 2-12 independent experiments performed with triplicate samples (error bars represent S.E.M), and summary data are presented in Table 1.

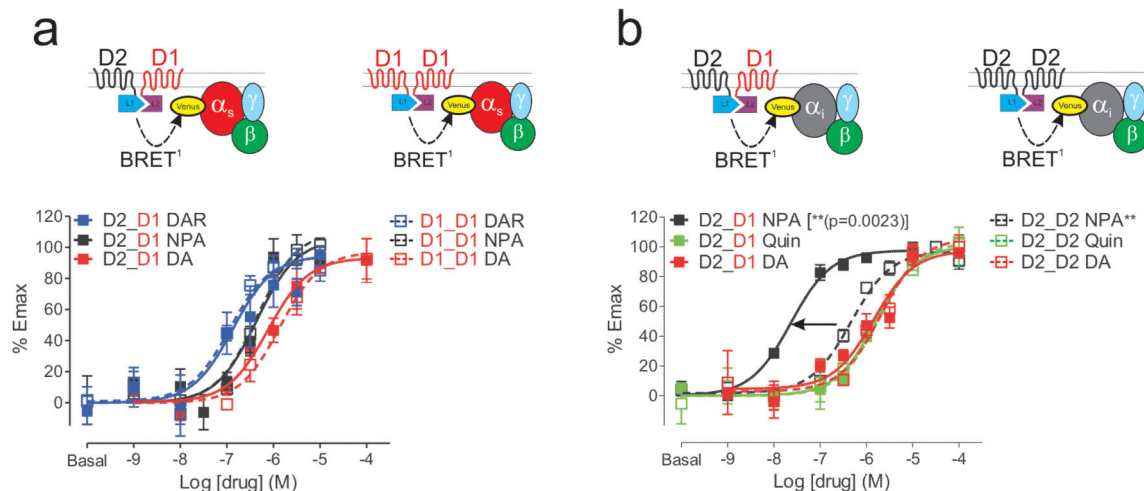


**Figure 4. CODA-RET reveals functional selectivity of NPA at the D2R-D1R heteromer**  
 HEK 293T cells coexpressing D1R-L1 and D1R-L2 or D2R-L1 and D1R-L2 together with G $\alpha$ <sub>s</sub>-mVenus (**a**) or D2R-L1 and D2R-L2 or D2R-L1 and D1R-L2 together with G $\alpha$ <sub>i</sub>-mVenus (**b**) were prepared as described in Figure 1. BRET<sup>1</sup> was measured as explained in Material and Methods and analyzed as for Figure 1 and EC<sub>50</sub> values were calculated after normalization (% of maximal BRET<sup>1</sup> signal) and application of global sigmoidal dose-response fitting with shared values for basal, EC<sub>50</sub> and Emax. The graphs are representative of at 2-12 independent experiments performed with triplicate samples (error bars represent S.E.M).

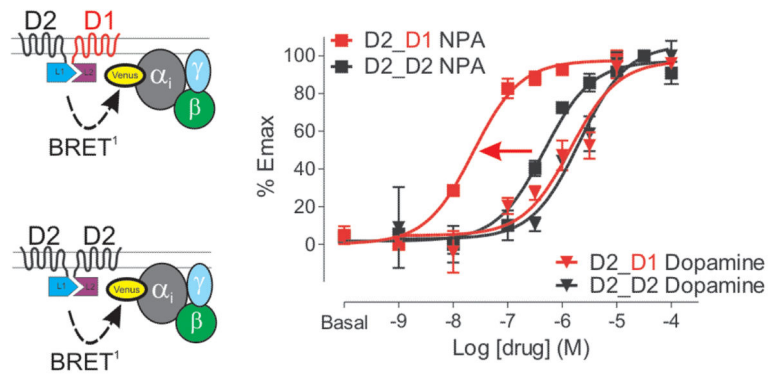


Figure 5.

Author Manuscript

Author Manuscript

Author Manuscript

Author Manuscript

**Table 1**  
**Characterization of D1R, D2R homo- and heteromers**

Receptor	G protein	Treatment	EC <sub>50</sub> (Mean±SD) (M)	n
D1R-RLuc8	Gas-mVenus	NPA	3.01×10 <sup>-6</sup> ±6.87×10 <sup>-7</sup>	2
D1R-RLuc8 + D2R		NPA	1.49×10 <sup>-6</sup> ±3.50×10 <sup>-7</sup>	2
D2R-RLuc8	Gai-mVenus	Quinpirole	1.14×10 <sup>-6</sup> ±4.11×10 <sup>-7</sup>	3
		NPA ***	3.60×10 <sup>-7</sup> ±7.70×10 <sup>-8</sup>	4
D2R-RLuc8 + D1R	Gai-mVenus	Quinpirole	1.20×10 <sup>-6</sup> ±3.17×10 <sup>-7</sup>	3
		NPA ***	2.02×10 <sup>-8</sup> ±7.55×10 <sup>-9</sup>	4
D1R-L1 + D1R-L2	Gas-mVenus	Dopamine	1.41×10 <sup>-6</sup> ±4.24×10 <sup>-7</sup>	3
		Dopamine+SCH23390	NF	3
		DAR100	2.02×10 <sup>-7</sup> ±1.04×10 <sup>-7</sup>	3
		SKF83822	1.07×10 <sup>-7</sup> ±3.24×10 <sup>-8</sup>	6
		NPA	2.51×10 <sup>-7</sup> ±1.79×10 <sup>-7</sup>	3
D2R-L1 + D2R-L2	Gai-mVenus	Dopamine	2.27×10 <sup>-6</sup> ±7.61×10 <sup>-7</sup>	4
		Dopamine+Sulpiride	NF	2
		Quinpirole	1.66×10 <sup>-6</sup> ±9.24×10 <sup>-7</sup>	9
		NPA **	1.98×10 <sup>-7</sup> ±1.49×10 <sup>-7</sup>	12
D2R-L1 + D1R-L2	Gas-mVenus	Dopamine	8.27×10 <sup>-7</sup> ±8.69×10 <sup>-8</sup>	2
		DAR100	1.18×10 <sup>-7</sup> ±7.92×10 <sup>-8</sup>	3
		SKF83822	1.78×10 <sup>-7</sup> ±5.72×10 <sup>-8</sup>	4
		SKF83822+Sulpiride	1.87×10 <sup>-7</sup> ±1.70×10 <sup>-9</sup>	2
		SKF83822+SCH23390	NF	3
		SKF81297	3.74×10 <sup>-8</sup> ±1.47×10 <sup>-8</sup>	6
		SKF81297+Sulpiride	3.34×10 <sup>-8</sup> ±3.74×10 <sup>-9</sup>	2
		SKF81297+SCH23390	NF	2
		SKF38393	3.59×10 <sup>-7</sup> ±9.54×10 <sup>-8</sup>	3
		SKF38393+Sulpiride	1.86×10 <sup>-7</sup> ±1.59×10 <sup>-7</sup>	2
		SKF38393+SCH23390	NF	2
D2R-L1 + D1R-L2	Gai-mVenus	Dopamine	1.24×10 <sup>-6</sup> ±4.51×10 <sup>-7</sup>	3
		Dopamine+Sulpiride	NF	2
		Dopamine+SCH23390	2.33×10 <sup>-6</sup> ±8.80×10 <sup>-7</sup>	2
		Quinpirole	1.16×10 <sup>-6</sup> ±5.03×10 <sup>-7</sup>	12
		Quinpirole+Sulpiride	NF	2
		Quinpirole+SCH23390	1.83×10 <sup>-6</sup> ±6.09×10 <sup>-7</sup>	5

Receptor	G protein	Treatment	EC <sub>50</sub> (Mean±SD) (M)	n
		NPA **	2.22×10 <sup>-8</sup> ±9.10×10 <sup>-9</sup>	9
		NPA+Sulpiride	2.52×10 <sup>-6</sup> ±8.59×10 <sup>-7</sup>	4
		NPA+SCH23390	6.14×10 <sup>-8</sup> ±3.31×10 <sup>-8</sup>	3

\*\*\*

p= 0.0001 (Unpaired t test, two tailed)

D2R-RLuc8 + Gai-mVenus NPA vs. D2R-RLuc8 + D1R Gai-mVenus NPA.

\*\*

p= 0.0023 (Unpaired t test, two tailed)

D2R-L1 + D2R-L2 + Gai-mVenus NPA vs. D2R-L1+ D1R-L2 + Gai-mVenus NPA.

**n**: number of independent experiments performed with triplicate samples

NF: not fit

Author Manuscript

Author Manuscript

Author Manuscript

Author Manuscript